# NCEP NOTES

## WSR-88D Radar Data Processing at NCEP

SHUN LIU,[a,b] GEOFF DIMEGO,[b] SHUCAI GUAN,[b] V. KRISHNA KUMAR,[c] DENNIS KEYSER,[b] QIN XU,[d] KANG NAI,[e] PENGFEI ZHANG,[e] LIPING LIU,[e,f] JIAN ZHANG,[d] KENNETH HOWARD,[d] AND JEFF ATOR[b]

[a] *I. M. Systems Group, Inc., Rockville, Maryland*
[b] *NOAA/National Centers of Environmental Prediction, College Park, Maryland*
[c] *Riverside Technology Inc., NOAA/NESDIS/JCSDA, College Park, Maryland*
[d] *NOAA/National Severe Storms Laboratory, Norman, Oklahoma*
[e] *Cooperative Institute for Mesoscale Meteorological Studies, University of Oklahoma, Norman, Oklahoma*
[f] *Chinese Academy of Meteorological Sciences, Beijing, China*

(Manuscript received 1 February 2016, in final form 12 July 2016)

ABSTRACT

Real-time access to level II radar data became available in May 2005 at the National Centers for Environmental Prediction (NCEP) Central Operations (NCO). Using these real-time data in operational data assimilation requires the data be processed reliably and efficiently through rigorous data quality controls. To this end, advanced radar data quality control techniques developed at the National Severe Storms Laboratory (NSSL) are combined into a comprehensive radar data processing system at NCEP. Techniques designed to create a high-resolution reflectivity mosaic developed at the NSSL are also adopted and installed within the NCEP radar data processing system to generate hourly 3D reflectivity mosaics and 2D-derived products. The processed radar radial velocity and 3D reflectivity mosaics are ingested into NCEP's data assimilation systems to improve operational numerical weather predictions. The 3D reflectivity mosaics and 2D-derived products are also used for verification of high-resolution numerical weather prediction. The NCEP radar data processing system is described.

## 1. Introduction

Doppler weather radar has the capability to scan a large volume of the atmosphere at high spatial and temporal resolutions. The network of Weather Surveillance Radars-1988 Doppler (WSR-88Ds) or Next Generation Weather Radar (NEXRAD) sites provides invaluable observations for observing atmospheric conditions at high resolution across the United States (Crum and Alberty 1993). The images from radar observations are successfully used to detect severe weather and warn of thunderstorms (Burgess 2004; Mitchell et al. 1998; Vasiloff 2001; Liu et al. 2007). The use of high-resolution radar data to improve numerical weather prediction (NWP) is also active in the academic and research communities. A number of algorithms have been developed over the years to initialize numerical prediction models by assimilating the radar reflectivity and/or radial wind observations. This body of research indicates that the utilization of radar data has great potential for improving NWP forecasts (Carley 2012; Dowell et al. 2011; Hu et al. 2006; Stensrud et al. 2009; Sun 2005; Xue et al. 2000).

However, progress in using high-resolution level II data in operational NWP models has been much slower than in research models over the years (Weygandt and Benjamin 2007; Alpert and Kumar 2007). The lack of progress may be attributable to key obstacles such as 1) difficulty in transmitting relatively large volumes of radar to the operational center in real time, 2) radar data decoding software and storage requiring an excessive amount of computational resources, 3) operational high-resolution storm-scale data assimilation systems using radar observations that require huge amounts of

*Corresponding author address*: Dr. Shun Liu, NOAA/NCWCP W/NP2, 5830 University Research Ct., College Park, MD 20740.
E-mail: shun.liu@noaa.gov

DOI: 10.1175/WAF-D-16-0003.1

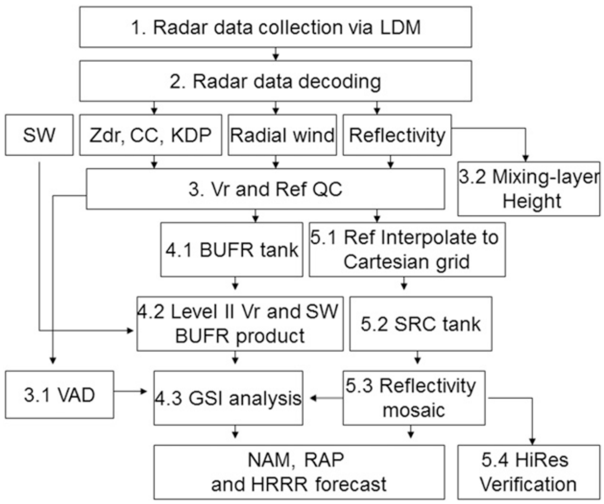


FIG. 1. Flowchart of WSR-88D radar data processing at NCEP.

computational resources, and 4) various radar data quality problems that can limit the application of radar data for operational use. Owing to the success of the Collaborative Radar Acquisition Field Test project (CRAFT; Droegemeier et al. 2002), the National Centers for Environmental Prediction (NCEP) have been accessing the level II data in real time from a network of 156 National Weather Service (NWS) WSR-88D radars since May 2005. The NCEP Central Operations (NCO) facility has assigned a dedicated node with 32 processors in the NCEP's operational supercomputing environment to process level II radar data in real time. With the addition of these computational and disk storage resources, the first two obstacles were overcome. Recently, NCEP has gradually begun to gain the ability to improve the regional model resolution in operations. Thus, an efficient system for processing the raw level II radar data must then be developed. This system should be reliable and efficient enough to remove radar data quality problems and provide level II radar data products that will support all relevant NCEP operational applications.

In this paper, the radar data processing system at NCEP is described in detail. A flowchart of the radar data processing process is introduced in section 2. The implementation of a quality control (QC) package is described in section 3. In addition, the performance of the QC package is examined in section 4 and a summary is provided in section 5.

## 2. Radar data processing at NCEP

The WSR-88D radar data processing system at NCEP comprises the following components outlined in the flowchart shown in Fig. 1. 1) The Local Data Management (LDM) system is used to receive compressed raw level II radar data at NCO. Once the data are received, they are uncompressed and decoded to obtain the radial wind (Vr), reflectivity at the horizontal polarization (Ref), spectrum width (SW), cross-correlation coefficient between the horizontally and vertically polarized radar return (CC), differential reflectivity (ZDR), and differential phase (KDP). 2) The uncompressed and decoded reflectivity data at 3.5° and 4.5° elevations are used to estimate the mixing-layer height based on "ring" features shown in the reflectivity (Heinselman et al. 2009). 3) Comprehensive QC is then performed to deal with various radar data quality problems (e.g., aliased radial winds, anomalous propagation, etc.). 4) For each volume scan, the quality controlled radial wind, reflectivity, and spectrum width data are stored in data tanks in Binary Universal Form for the Representation of Meteorological Data (BUFR) format as shown in step 4.1 in Fig. 1. The radial wind data are then written out every 3 h and assimilated by the North American Mesoscale (NAM) Data Assimilation System (NDAS). The radial wind data are also written out hourly and used for the Rapid Refresh (RAP) and High Resolution Rapid Refresh (HRRR) forecast systems as show in step 4.2 in Fig. 1. The quality controlled radial winds are further used to calculate velocity azimuth display (VAD) winds from each station. 5) Quality controlled reflectivity fields are interpolated from a radar polar grid onto a Cartesian grid via a single-radar Cartesian (SRC; J. Zhang et al. 2005) package. Gridded reflectivities from each volume scan are first put into a buffer area, then a 3D reflectivity mosaic package developed by National Severe Storms Laboratory (NSSL) is used to interpolate the 3D reflectivity product to a unified Cartesian coordinate with 1-km grid spacing and 31 vertical levels above the sea surface (500, 750, 1000, 1250, 1500, 1750, 2000, 2250, 2500, 2750, 3000, 3500, 4000, 4500, 5000, 5500, 6000, 6500, 7000, 7500, 8000, 8500, 9000, 10 000, 11 000, 12 000, 13 000, 14 000, 15 000, 16 000, and 18 000 m). The 2D-derived products are also computed from 3D reflectivity mosaics, which include composite reflectivity, echo top, and hybrid scan reflectivity (the column maximum reflectivity from the lowest two elevation scans). The 3D reflectivity products are used in data assimilation to help initialize ongoing convection in the operational RAP, HRRR, and NAM models using a diabatic digital filter initialization technique (Weygandt and Benjamin 2007). The derived products are also used for high-resolution verification at NCEP.

The whole WSR-88D radar data processing system has been found to be reliable and efficient in NCEP operations since its implementation in May 2005. In the above steps, the radar data QC algorithms have evolved over time and have had a beneficial impact on the robustness of the radar data used at NCEP. The NCEP QC algorithms will be discussed further in the next section.

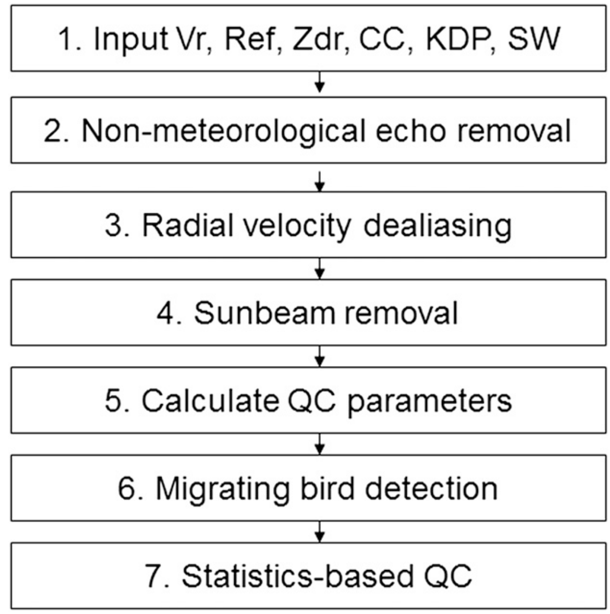


FIG. 2. Flowchart of WSR-88D radar data QC at NCEP.

## 3. Radar data quality control

Prototype real-time radar data QC algorithms developed by Liu et al. (2003) and Gong et al. (2003) have been improved and implemented into operations at NCEP beginning in May 2005. The radial velocity QC technique has been improved substantially through a series of adaptive upgrades (Xu 2009; Xu et al. 2004, 2009, 2010, 2011) and tested extensively at NSSL as well as in an operational environment at NCEP. The latest addition to the QC package is the use of dual-polarization (dual-pol) observations to improve the radial wind and reflectivity QC process. In particular, a new QC component for identifying nonmeteorological echoes using dual-pol observations (named dual-pol-based QC) was incorporated into the upgraded QC package at NCEP on 28 May 2013 (Jiang et al. 2013; Tang et al. 2014).

The radar data QC used at NCEP for processing real-time radar data is fully automatic and highly efficient. The QC techniques used at NCEP are different from those implemented at the Radar Operations Center (ROC). The radar data QC techniques implemented at ROC were developed primarily for visual and qualitative applications with considerable tolerance for bad or poor quality data, to retain as much of the original data coverage as possible. These processed data do not satisfy the high quality standard required by operational data assimilation at NCEP. In the research community, radar data assimilation has been more or less limited to case studies where mixed objective and subjective radar data QC techniques are often used. Sometimes, even manual editing and cleaning are involved in the radar data processing to ensure the data is free of quality problems. Such manual QC approaches are clearly not suitable for NCEP's operational data assimilation. It is necessary and critical to develop automated, high-standard QC techniques to ensure that the processed radar data are free of quality problems and thus can be assimilated into the NCEP's operational NWP systems.

A flowchart of the NCEP radar data QC process is shown in Fig. 2. The key functionalities of the NCEP radar data QC involve seven steps for detecting and correcting or removing unqualified radar observations in operations. 1) The super-resolution ($0.5° \times 250$ m) raw level II data are recombined to the legacy resolution ($1° \times 250$ m for radial winds, spectrum width, and dual-pol variables and $1° \times 1000$ m for reflectivity). All of the above radar-observed variables are input into the QC software package. The raw data recombination reduces the usage of computation resources in operational radar data processing and meets the current needs of radar data applications at NCEP. 2) Initially, a fuzzy-logic-based algorithm (Liu et al. 2008) was used to detect and remove ground clutter and sea clutter from the observed radial wind and reflectivity fields. After the entire WSR-88D network was upgraded with dual-pol capability, a fuzzy-logic-based QC algorithm using three dual-pol variables was developed to identify nonmeteorological echoes (Jiang et al. 2013; Tang et al. 2014). 3) After nonmeteorological echo removal, an advanced radial velocity dealiasing algorithm based primarily on the work of Xu et al. (2011) is then used to correct or remove aliased radial velocities. 4) A Sunbeam filter is applied to remove unqualified returns, called sun spikes, when the antenna of a radar is aimed at the sun. A sun spike is displayed as a narrow ray of the returned energy along the radial direction and can be removed by detecting the discontinuity of the radar returns along the azimuth (Lakshmanan et al. 2007). 5) After the above steps, the following QC statistical parameters used in P. Zhang et al. (2005) on each tilt are calculated: (i) the standard deviation of the radial wind (STD), (ii) the percentage of the radial wind sign change (SC) along the radial direction, (iii) the mean reflectivity on a tilt (MRF), (iv) the percentage of the along-beam perturbation velocity sign changes (PSCs), and (v) the radial velocity data coverage (VDC). 6) The QC parameters from step 5

TABLE 1. Thresholds of QC parameters.

| QC threshold | STD | SC | MRF | PSC | VDC |
|---|---|---|---|---|---|
| Max threshold | 2.75 | 17.5 | 11.0 | 38 | 10 |
| Min threshold | 0 | 0 | −2 | 0 | 0 |

above are then subsequently used to identify migrating birds with the Bayesian method developed by P. Zhang et al. (2005) and Liu et al. (2005). However, since the newly developed dual-pol-based QC has been tested and found to be very efficient and effective on identifying biological echoes, the new version of migrating bird detection relies mainly on the dual-pol-based QC method. The Bayesian method is still performed as a sanity check in case the dual-pol data are not available. 7) Finally, the above five QC parameters are further used to statistically eliminate noisy and other poor-quality data via the use of the probability density function (pdf) estimated from a histogram for each QC parameter. If the value calculated on a tilt for any of the five QC parameters falls outside the range of significant probability, the data on that tilt are rejected. The radial wind and reflectivity that pass through all seven QC steps (Fig. 2) are further used by NCEP's operational NWP systems (e.g., the NAM) as shown steps 4.3 and 5.3 in Fig. 1.

Because the method used in step 7 (Fig. 2) was not previously published or reported, the technical details of this step are described here with illustrative examples. Values of the five QC parameters are calculated and accumulated from 18 March to 20 May 2007. The accumulated values are then used to generate histograms for the five QC parameters. The pdf of a QC parameter can be estimated from the histogram of that QC parameter (Liu et al. 2005). The maximum and minimum thresholds for each QC parameter are empirically determined to cover the range of significant probabilities based on the pdf of that QC parameter. If the calculated value of any QC parameter from the radar data on a given tilt is not between the maximum and minimum thresholds, then the radar data on that tilt will be rejected. The empirically determined thresholds are listed for each QC parameter in Table 1.

An example of a histogram of SC is shown in Fig. 3. For this QC parameter, the maximum threshold used to reject the data is 20%, as indicated by the black line. Figure 4a displays the level II radial wind imagery scanned from precipitation at 0.5° elevation by the Dallas/Fort Worth, Texas (KFWS), radar at 0605 UTC 11 September 2009, while Fig. 4b displays the radial wind imagery from clear-sky scans at 0.5° elevation by the Buffalo, New York (KBUF), radar at 1325 UTC 9 September 2009. The SC value calculated from the radial wind field in Fig. 4a is merely 6.5%, while the SC

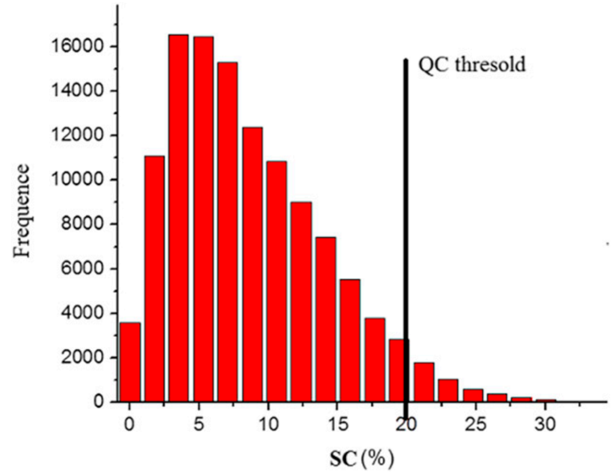


FIG. 3. Histogram of the percentage of radial wind sign change along the radial direction.

value calculated from the radial wind field in Fig. 4b is 23.0%. Clearly, the clear-sky radial winds in Fig. 4b are much noisier than those observed from precipitation in Fig. 4a. The data in Fig. 4b are thus rejected by the statistically based QC method used in step 7 above. The performance of the whole QC package will be examined in the next section.

## 4. Performance of radar data QC

### *a. Radial wind QC*

Since there are many conventional wind observations available operationally at NCEP from instruments other than radars (such as rawinsondes, profilers, aircraft, etc.), and the radar radial wind observation operator used in the variational data assimilation system is simple and linear, it is relatively easy to examine the performance of the radial wind QC objectively by using other independent observations. Wind analysis using the 12-km NAM forecast system, which employs the Gridpoint Statistical Interpolation (GSI) data assimilation package (Wu et al. 2002), is first performed with all operationally used observational data except for those for the radial wind. The analyzed winds are used as reference winds to examine the performance of the radial wind QC. Reference winds are projected onto the radial directions at the radial wind observation locations by utilizing the forward operator for the radial wind observations from the GSI variational data assimilation system. Scatterplots of radar radial winds of observed radar radial winds versus referenced radar radial winds are shown in Figs. 5a,b. If the observed radial winds agree with the reference radial winds, the plotted data points will fall near and equally on either side of the

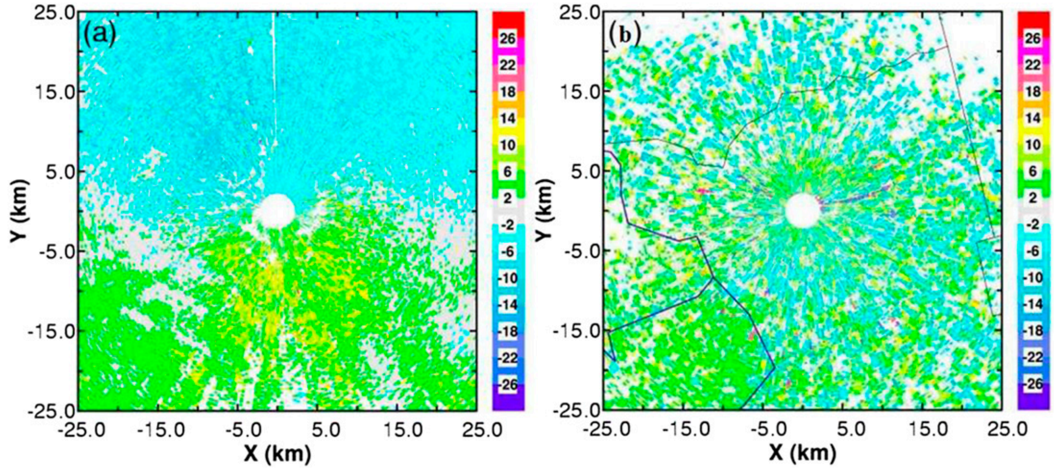


FIG. 4. Radial wind observations ($m\,s^{-1}$) at 0.5° elevation collected by (a) KFWS at 0605 UTC 9 Sep 2009 and (b) KBUF at 1325 UTC 5 Sep 2009.

diagonal line. In an idealized situation, the plotted data points will fall on the line of equality in the figure. If the plotted data points deviate significantly from the line of best fit, a large bias exists between the observed and reference radial winds. Clearly, the data points are scattered more broadly before QC (Fig. 5a) than after QC (Fig. 5b). In particular, very large differences ($>20\,m\,s^{-1}$) between the observed and reference radial winds are seen in the top-left corner and the bottom-right corner of Fig. 5a. The large differences are caused mainly by alias errors in the raw radial winds. Thus, assimilating the raw radial winds without QC directly into an NWP model has a high potential for degrading the forecast skill. Large differences are also seen around the vertical line of zero value for the observed radial wind, which are caused mainly by ground or sea clutter in the returned echoes. After QC, most of the data points with a large deviation in Fig. 5a are eliminated in Fig. 5b, so the biases between the observed and reference radial winds have been reduced considerably after QC. Some of selected data points with a large deviation are further examined by plotting the radial wind image at the corresponding elevation. As indicated by various diagnostics of radial wind images, the current radial wind QC package performs reasonably well in rejecting unqualified data.

### b. Reflectivity QC

Deriving radar reflectivity data directly from other sources of observations in operations is currently not feasible, which inhibits our ability to apply a direct and quantifiable method for examining the performance of

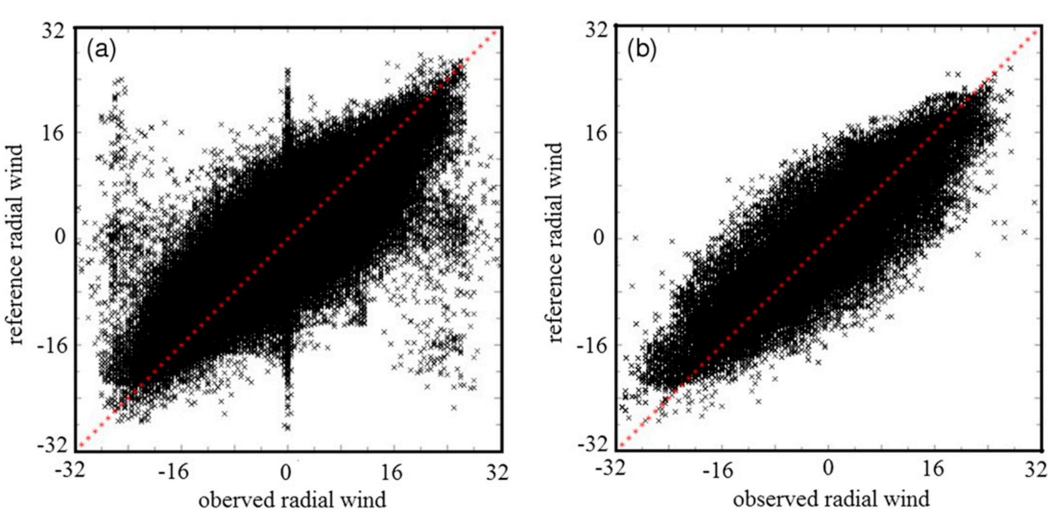


FIG. 5. Scatterplots of radial wind ($m\,s^{-1}$) (a) before and (b) after QC.

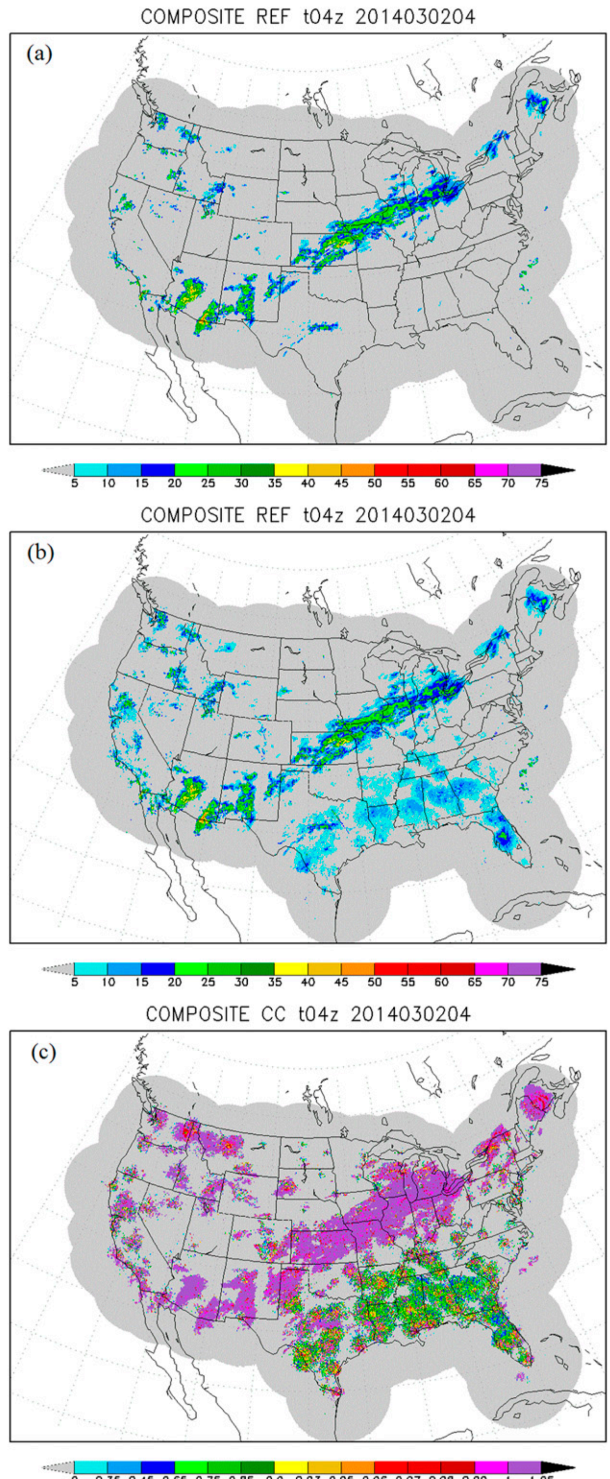


FIG. 6. Composite reflectivity (dB$Z$) (a) before and (b) after QC and (c) composite dual-pol variable CC at 0400 UTC 2 Mar 2014.

radar reflectivity QC within the framework of current operational datasets. The performance of reflectivity QC is evaluated mainly by human expertise in operations. For a case study, an objective evaluation algorithm is also developed to evaluate the quality of the derived products from the 3D reflectivity products.

To facilitate continued evaluation from human experts, images of composite reflectivity from the quality controlled 3D reflectivity mosaic are displayed in real time on NCEP's radar data monitoring web page. The performance of reflectivity QC is then monitored by NCEP and NOAA/Global Systems Division users. Based on the feedback from users, the current QC is able to reject most of the contaminated or unqualified reflectivity data.

With the dual-pol technology upgrade across the WSR-88D radar network, offline dual-pol products are also developed to help human experts examine and monitor reflectivity quality. For example, column maximum CC and ZDR (named as composite CC and composite ZDR) are derived as needed. The three-dimensional CC and ZDR results are projected onto a two-dimensional grid in a manner that is analogous to what is done to obtain composite radar reflectivity. The images of the two products are generated and displayed on NCEP's radar data monitoring web page. Since composite CC and ZDR show obvious differences between the meteorological echo area and the nonmeteorological echo area, experts can easily identify if the major nonmeteorological echoes are removed in the 3D reflectivity mosaic. Thus, these dual-pol variables, in addition to being used to help remove nonmeteorological echoes in the automated QC procedure, also facilitate continued, interactive monitoring of the reflectivity QC system.

An example of composite reflectivity with and without reflectivity QC at 0400 UTC 2 March 2014 is shown in Figs. 6a,b. The corresponding composite CC is shown in Fig. 6c. Without reflectivity QC, blue-disk-like echoes emerge throughout the southeast of the continental United States, as shown in Fig. 6b. This may be caused by clear-air echoes or nonmeteorological echoes (P. Zhang et al. 2005; Liu et al. 2005). The composite CC is shown in Fig. 6c. It is clear that the composite CC is less than 0.9 (Lakshmanan et al. 2014) within the region of nonmeteorological echoes (i.e., the southeastern United States). In Fig. 6b, the application of the QC package eliminates most of the contaminated or unqualified data while retaining most of the physical or meteorological echoes.

To further objectively evaluate the performance of reflectivity QC, the cloud coverage product developed by the NASA Langley cloud and radiation research

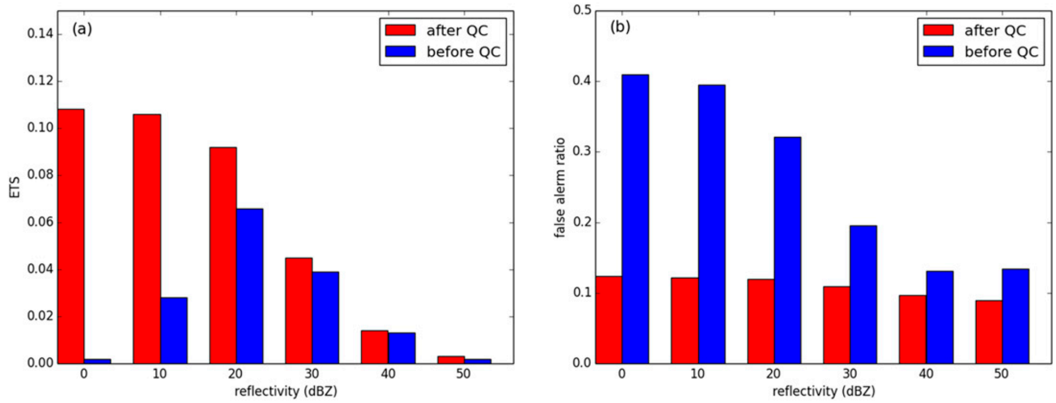


FIG. 7. ETS of composite radar reflectivity coverage against cloud coverage derived from (a) satellite observations and (b) the false alarm ratio before and after QC from 10 to 17 Sep 2014.

group (http://www-pm.larc.nasa.gov/) is compared with the reflectivity coverage results (Lakshmanan et al. 2007). The meteorological echoes observed by radar show good correspondence with the cloud coverage. The cloud coverage at the same location as the observed reflectivity can be used to identify meteorological and nonmeteorological echoes. The radar reflectivity coverage results before and after QC at 0000, 0600, 1200, and 1800 UTC from 10 to 17 September 2014 are derived from composite reflectivity. The equitable threat score (ETS) and false alarm ratio of the radar reflectivity coverage corresponding to cloud coverage are calculated and shown in Fig. 7. The ETS scores before QC (Fig. 7a) are clearly lower than those after QC and in the range 0–20 dB$Z$. The false alarm ratios before QC are also higher than after QC in Fig. 7b. The low ETS scores and high false alarm ratios before QC in the range 0–20 dB$Z$ are caused by nonmeteorological echoes, as shown in Fig. 6a.

As shown above, both subjective evaluation by experts and objective verification of reflectivity coverage against cloud coverage indicate that current reflectivity QC can effectively reject nonmeteorological echoes.

## 5. Summary and future work

Key characteristics of the WSR-88D radar data processing algorithms at NCEP have been reported in detail. The whole radar data process procedure is introduced by means of a flowchart. The QC algorithm used for radar radial wind and reflectivity in operations is described. The performance of radar radial wind QC is examined by comparing radar radial wind observations with the analyzed wind using all available observations. The results show that radial wind QC can reasonably reject unqualified data. The performance of the radar reflectivity QC is evaluated by subjective methods as well as objective methods. The current reflectivity QC can effectively reject nonmeteorological echoes.

Most of the components in the data processing system have been implemented in operations for more than eight years. The data processing system has been proven to be efficient and effective. However, the radar data QC process in the system is not perfect and there is room for further improvement in the radial wind and reflectivity QC by using other observations as part of the QC procedure (e.g., satellite images). In addition, NCEP has recently gained access to Canadian radar data from 13 stations and will gain access to Terminal Doppler Weather Radar (TDWR) radar data from 46 stations in the near future. As a result of different types of radar hardware, the scan patterns used and QC problems encountered with Canadian radars and TDWR radars differ from those in the operational WSR-88D radars. Processing these new data will require enhancements in computing power, disk storage, and the data flow network. It will also require upgrades to the existing radar data QC capabilities or even the development of new QC algorithms. All these issues pose new challenges to the NCEP radar data processing system and product line. Thus, continued efforts are required to further improve the radar data processing system at NCEP.

In 2016, the QC package is to be upgraded adaptively by incorporating the dealiasing technique developed for radial velocities scanned with small Nyquist velocities (Xu and Nai 2012, 2013). The new dealiasing method will be tested and implemented later at NCEP. Also, current NCEP's radar data processing will be combined with NSSL's Multiradar Multisensor System (MRMS).

*Acknowledgments.* The authors thank Mrs. Mary Hart for her careful editorial review and Dr. Jacob Carley for proofreading the manuscript and his valuable comments. This work was completed at the National Centers for Environmental Prediction. The work was also supported by the NOAA/NSSL Warn-on-Forecast project and ONR Grant N000141410281 to the University of Oklahoma (OU).

## REFERENCES

Alpert, J., and V. K. Kumar, 2007: Radial wind super-obs from the WSR-88D radars in the NCEP operational assimilation system. *Mon. Wea. Rev.*, **135**, 1090–1109, doi:10.1175/MWR3324.1.

Burgess, D. W., 2004: High resolution analyses of the 8 May 2003 Oklahoma City storm. Part I: Storm structure and evolution from radar data. Preprints, *22nd Conf. on Severe Local Storms*, Hyannis, MA, Amer. Meteor. Soc., 12.4. [Available online at https://ams.confex.com/ams/11aram22sls/techprogram/paper_81939.htm.]

Carley, J. R., 2012: Hybrid ensemble-3DVar radar data assimilation for the short-term prediction of convective storms. Ph.D. thesis, Purdue University, 206 pp. [Available online at http://docs.lib.purdue.edu/dissertations/AAI3544029/.]

Crum, T. D., and L. Alberty, 1993: The WSR-88D and the WSR-88D Operational Support Facility. *Bull. Amer. Meteor. Soc.*, **74**, 1669–1687, doi:10.1175/1520-0477(1993)074<1669:TWATWO>2.0.CO;2.

Dowell, D. C., L. J. Wicker, and C. Snyder, 2011: Ensemble Kalman filter assimilation of radar observations of the 8 May 2003 Oklahoma City supercell: Influences of reflectivity observations on storm-scale analyses. *Mon. Wea. Rev.*, **139**, 272–294, doi:10.1175/2010MWR3438.1.

Droegemeier, K. K., and Coauthors, 2002: Project CRAFT: A test bed for demonstrating the real time acquisition and archival of WSR-88D level II data. Preprints, *18th Int. Conf. on Interactive Information Processing Systems (IIPS) for Meteorology, Oceanography, and Hydrology*, Orlando, FL, Amer. Meteor. Soc., 136–139.

Gong, J., L. Wang, and Q. Xu, 2003: A three-step dealiasing method for Doppler velocity data quality control. *J. Atmos. Oceanic Technol.*, **20**, 1738–1748, doi:10.1175/1520-0426(2003)020<1738:ATDMFD>2.0.CO;2.

Heinselman, P. L., D. J. Stensrud, R. M. Hluchan, P. L. Spencer, P. C. Burke, and K. L. Elmore, 2009: Radar reflectivity–based estimates of mixed layer depth. *J. Atmos. Oceanic Technol.*, **26**, 229–239, doi:10.1175/2008JTECHA1091.1.

Hu, M., M. Xue, and K. Brewster, 2006: 3DVAR and cloud analysis with WSR-88D level II data for the prediction of the Fort Worth, Texas, tornadic thunderstorms. Part I: Cloud analysis and its impact. *Mon. Wea. Rev.*, **134**, 675–698, doi:10.1175/MWR3092.1.

Jiang, Y., Q. Xu, P. Zhang, and L. Liu, 2013: Using WSR-88D polarimetric data to identify bird-contaminated Doppler velocity. *Adv. Meteor.*, **2013**, 769275, doi:10.1155/2013/769275.

Lakshmanan, V., A. Fritz, T. Smith, K. Hondl, and G. Stumpf, 2007: An automated technique to quality control radar reflectivity data. *J. Appl. Meteor. Climatol.*, **46**, 288–305, doi:10.1175/JAM2460.1.

——, C. Karstens, J. Krause, and L. Tang, 2014: Quality control of weather radar data using polarimetric variables. *J. Atmos. Oceanic Technol.*, **31**, 1234–1249, doi:10.1175/JTECH-D-13-00073.1.

Liu, L., Q. Xu, P. Zhang, and S. Liu, 2008: Automated detection of contaminated radar image pixels in mountain areas. *Adv. Atmos. Sci.*, **25**, 778–790, doi:10.1007/s00376-008-0778-x.

Liu, S., P. Zhang, L. Wang, J. Gong, and Q. Xu, 2003: Problems and solutions in real-time Doppler wind retrievals. Preprints, *31th Conf. on Radar Meteorology*, Seattle, WA, Amer. Meteor. Soc., P2C.6. [Available online at https://ams.confex.com/ams/pdfpapers/63754.pdf.]

——, Q. Xu, and P. Zhang, 2005: Identifying Doppler velocity contamination caused by migrating birds. Part II: Bayes identification and probability tests. *J. Atmos. Oceanic Technol.*, **22**, 1114–1121, doi:10.1175/JTECH1758.1.

——, M. Xue, and Q. Xu, 2007: Using wavelet analysis to detect tornadoes from Doppler radar radial-velocity observations. *J. Atmos. Oceanic Technol.*, **24**, 344–359, doi:10.1175/JTECH1989.1.

Mitchell, E. D., S. V. Vasiloff, G. J. Stumpf, A. Witt, M. D. Eilts, J. T. Johnson, and K. W. Thomas, 1998: The National Severe Storms Laboratory tornado detection algorithm. *Wea. Forecasting*, **13**, 352–360, doi:10.1175/1520-0434(1998)013<0352:TNSSLT>2.0.CO;2.

Stensrud, D. J., and Coauthors, 2009: Convective-scale warn-on-forecast system: A vision for 2020. *Bull. Amer. Meteor. Soc.*, **90**, 1487–1499, doi:10.1175/2009BAMS2795.1.

Sun, J., 2005: Convective-scale assimilation of radar data: Progress and challenges. *Quart. J. Roy. Meteor. Soc.*, **131**, 3439–3463, doi:10.1256/qj.05.149.

Tang, L., J. Zhang, C. Langston, J. Krause, K. Howard, and V. Lakeshmana, 2014: A physically based precipitation–nonprecipitation radar echo classifier using polarimetric and environmental data in a real-time national system. *Wea. Forecasting*, **29**, 1106–1119, doi:10.1175/WAF-D-13-00072.1.

Vasiloff, V. S., 2001: Improving tornado warnings with the Federal Aviation Administration's Terminal Doppler Weather Radar. *Bull. Amer. Meteor. Soc.*, **82**, 861–874, doi:10.1175/1520-0477(2001)082<0861:ITWWTF>2.3.CO;2.

Weygandt, S. S., and S. Benjamin, 2007: Radar reflectivity-based initialization of precipitation systems using a diabatic digital filter within rapid update cycle. Preprints, *18th Conf. on Numerical Weather Prediction*, Park City, UT, Amer. Meteor. Soc., 1B.7. [Available online at https://ams.confex.com/ams/22WAF18NWP/techprogram/paper_124540.htm.]

Wu, W.-S., R. J. Purser, and D. F. Parrish, 2002: Three-dimensional variational analysis with spatially inhomogeneous covariances. *Mon. Wea. Rev.*, **130**, 2905–2916, doi:10.1175/1520-0493(2002)130<2905:TDVAWS>2.0.CO;2.

Xu, Q., 2009: Bayesian perspective of the unconventional approach for assimilating aliased radar radial velocities. *Tellus*, **61A**, 631–634, doi:10.1111/j.1600-0870.2009.00413.x.

——, and K. Nai, 2012: An adaptive dealiasing method based on variational analysis for radar radial velocities scanned with small Nyquist velocities. *J. Atmos. Oceanic Technol.*, **29**, 1723–1729, doi:10.1175/JTECH-D-12-00145.1.

——, and ——, 2013: A two-step variational method for analyzing severely aliased radar velocity observations with small Nyquist velocities. *Quart. J. Roy. Meteor. Soc.*, **139**, 1904–1911, doi:10.1002/qj.2075.

——, L. Wang, P. Zhang, S. Liu, Q. Zhao, K. Sashegyi, and J. Nachamkin, 2004: Progress in radar data quality control and assimilation. Preprints, *Sixth Int. Symp. on Hydrological Applications of Weather Radar*, Melbourne, VIC, Australia, Australian Bureau of Meteorology.

——, K. Nai, L. Wei, and Q. Zhao, 2009: An unconventional approach for assimilating aliased radar radial velocities. *Tellus*, **61A**, 621–630, doi:10.1111/j.1600-0870.2009.00412.x.

——, ——, and ——, 2010: Fitting VAD wind to aliased Doppler radial-velocity observations: A minimization problem with multiple minima. *Quart. J. Roy. Meteor. Soc.*, **136**, 451–461, doi:10.1002/qj.589.

——, ——, ——, P. Zhang, S. Liu, and D. Parrish, 2011: A VAD-based dealiasing method for radar velocity data quality control. *J. Atmos. Oceanic Technol.*, **28**, 50–62, doi:10.1175/2010JTECHA1444.1.

Xue, M., K. K. Droegemeier, and V. Wong, 2000: The Advanced Regional Prediction System (ARPS)—A multiscale nonhydrostatic atmospheric simulation and prediction tool. Part I: Model dynamics and verification. *Meteor. Atmos. Phys.*, **75**, 161–193, doi:10.1007/s007030070003.

Zhang, J., K. Howard, and J. Gourley, 2005: Constructing three-dimensional multiple-radar reflectivity mosaics: Examples of convective storms and stratiform rain echoes. *J. Atmos. Oceanic Technol.*, **22**, 30–42, doi:10.1175/JTECH-1689.1.

Zhang, P., S. Liu, and Q. Xu, 2005: Identifying Doppler velocity contamination caused by migrating birds. Part I: Feature extraction and quantification. *J. Atmos. Oceanic Technol.*, **22**, 1105–1113, doi:10.1175/JTECH1757.1.